

Pose-Diversified Augmentation with Diffusion Model for Person Re-Identification

Inès Hyeonsu Kim^{*1} JungBin Lee^{*1} Soowon Son¹ Woojeong Jin¹
 Kyusun Cho¹ Junyoung Seo¹ Min-Seop Kwak¹ Seokju Cho¹
 JeongYeol Baek² Byeongwon Lee² Seungryong Kim¹

¹Korea University ²SKT



Figure 1: **Teaser:** Generated samples from a reference identity by **Diff-ID**. Our method can generate new human images conditioned on various poses while maintaining the appearance of the original human identity, which are used for augmenting the training data for person re-identification (Re-ID) task. Ref. denotes the reference image.

Abstract

Person re-identification (Re-ID) often faces challenges due to variations in human poses and camera viewpoints, which significantly affect the appearance of individuals across images. Existing datasets frequently lack diversity and scalability in these aspects, hindering the generalization of Re-ID models to new camera systems. Previous methods have attempted to address these issues through data augmentation; however, they rely on human poses already present in the training dataset, failing to effectively reduce the human pose bias in the dataset. We propose **Diff-ID**, a novel data augmentation approach that incorporates sparse and underrepresented human pose and camera viewpoint examples into the training data, addressing the limited diversity in the original training data distribution. Our objective is to augment a training dataset that enables existing Re-ID models to learn features unbiased by human pose and camera viewpoint variations. To achieve this, we leverage the knowledge of pre-trained large-scale diffusion models. Using the SMPL model, we simultaneously capture both the desired human poses and camera viewpoints, enabling realistic human rendering. The depth information provided by the SMPL model indirectly conveys the camera viewpoints. By conditioning the diffusion model on both the human pose and camera viewpoint concurrently through the SMPL model, we generate realistic images with diverse human poses and camera viewpoints. Qualitative results demonstrate the effectiveness of our

^{*}Equal contribution

method in addressing human pose bias and enhancing the generalizability of Re-ID models compared to other data augmentation-based Re-ID approaches. The performance gains achieved by training Re-ID models on our offline augmented dataset highlight the potential of our proposed framework in improving the scalability and generalizability of person Re-ID models. The project page is available at <https://ku-cvlab.github.io/Diff-ID/>.

1 Introduction

Person re-identification (Re-ID) has been popularly used to retrieve [67] and track [53] individuals across images captured by multiple cameras with non-overlapping views [6, 66]. It has applications in various fields, such as robotics [8] and surveillance [53].

However, real-world deployment of Re-ID often faces several challenges. A major obstacle arises from the differences in *human pose* [7, 45, 63] and *camera viewpoint* [1, 27] within images of the same individual. These variations significantly affect the appearance of individuals, making the identification task difficult. To overcome this, existing models often require diverse images, but datasets for Re-ID are limited in terms of scalability and generalizability [10], since manual labeling of individuals across cameras is notoriously challenging [34, 64]. Furthermore, the limited number of cameras in the datasets makes it challenging to generalize models to new camera networks [37, 53, 72]. As a result, learning pose-invariant features for Re-ID that remain consistent across different human poses and camera viewpoints remains a challenge.

To address these challenges, previous attempts [9, 10, 13, 24, 33, 38, 69, 70, 73] have involved data augmentation aimed at increasing the diversity of training data. Early methods employed simple image transformation techniques [24, 38, 73], while more recent approaches leverage generative adversarial networks (GAN)-based models for augmentation [33, 69, 70]. However, since these methods rely on poses already existing in the Re-ID dataset to generate augmented images, they do not effectively address the core issue of pose bias in the training data distribution. Even in the case that the human pose is the same, differences in camera angles may induce significant changes in appearance [57]. For example, a picture taken from a high-angle camera viewpoint may appear different from one taken from a low-angle viewpoint, potentially causing the same person to be identified as different individuals. To generalize and reduce the training data bias, it is crucial to diversify the training data’s human pose and camera viewpoint distribution.

In this paper, we define a novel pose augmentation techniques to consider both human pose and camera viewpoint. We propose a diffusion model-based framework, called **Diff-ID**, to augment the training data with poses and camera viewpoints that are underrepresented, *i.e.*, rarely appeared, in the original training dataset. By including these less common examples, we aim to minimize the impact of pose and viewpoint variations on appearance. This approach focuses to generalize the distribution of the training dataset, enabling the training of more scalable and generalizable Re-ID models. Furthermore, our model architecture is designed to consider both human pose and camera viewpoint, acknowledging their joint influence on a person’s appearance in Re-ID.

However, generating new images from sparse and limited poses is a challenging task. Since generative models learn the training data distribution, they may struggle to generate images with infrequently seen poses in the training data distribution, even if they are well-trained on a Re-ID dataset. To address this issue, we leverage Stable Diffusion [42], a pre-trained large-scale generative model, to augment our data with images of sparse and limited poses. By effectively leveraging the pre-trained knowledge, we can successfully augment the data, even when the given human pose and camera condition are uncommon in the training dataset. Also, to jointly provide human pose and camera viewpoint that are rarely seen in the training dataset, we use the SMPL [35] model. We conditioned the generative model with SMPL, enabling realistic human rendering and providing implicit information about the camera viewpoint through depth data.

Our objective is not developing a new Re-ID model, but rather augmenting a training dataset that enables Re-ID models to learn features unbiased to pose variations. We present performance gains achieved by training the Re-ID model on our offline augmented dataset using our proposed architecture. Furthermore, qualitative results demonstrate that, compared to other approaches, our architecture generates significantly more realistic and feasible images for human poses and viewpoints

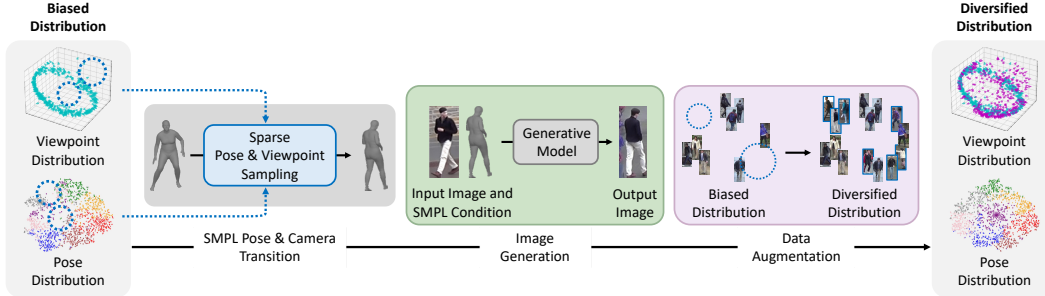


Figure 2: **Intuition of our framework.** Upon observing the highly biased viewpoint and human pose distributions in training dataset, we augment the dataset by manipulating SMPL body shapes and feeding the rendered shapes into a generative model to fill in sparsely distributed poses and viewpoints. With this augmented dataset, we can train a Re-ID model that is robust to viewpoint and human pose biases.

that were not well-represented in existing Re-ID models. This highlights the effectiveness of our method in addressing the pose bias issue and enhancing the generalizability of Re-ID models.

2 Related Work

Person re-identification. Person Re-ID is a crucial task in computer vision that involves identifying individuals across different camera views. Recent advancements in Re-ID [5, 10, 14, 19, 26, 31, 46, 51, 54] leverage deep learning techniques to improve Re-ID performance. The most significant method is Distance Metric Learning [20, 30, 32, 55, 58, 68], such as Triplet Loss [22], which utilizes deep learning models to project images into a feature embedding space where the vectors of the same identity are close together, while those of different identities are far apart.

Data augmentation in re-identification. Various approaches [9, 38, 24, 39, 70, 33, 69, 73] employed data augmentation techniques to enhance person Re-ID models. Operations such as random resizing, cropping, and horizontal flipping [38], along with adversarially occluded samples [24], increase the diversity of training data. Approaches using methods such as DropBlock [9] and background transformation [39] show further improved feature learning. Meanwhile, there are approaches [70, 33, 69] using a generative model, which is Generative Adversarial Networks (GANs) [15], for data augmentation in Re-ID task. DCGANs [70] generate new samples, enriching training datasets which improves the performance of the Re-ID model. [33] utilizes a data augmentation method involving pose-transferred sample augmentations. In [69], data augmentation is achieved through a joint learning framework that couples generative and discriminative modules. Techniques like random erasing [73] can also improve model robustness and generalization.

Pose-conditioned diffusion models. Pose-guided person image generation task aims to generate a person’s image with a specific pose. With the promising result of diffusion model [21, 48], there have been approaches [2, 61, 42, 17, 23, 28, 56, 75] that aim to generate human images with desired structure by applying diffusion model with 2D human pose as a condition. PIDM [2] is the first method that integrates the diffusion model [21, 48] pose-guided person synthesis task, using OpenPose [3] as the pose condition. ControlNet [61] takes a method to fine-tune Stable Diffusion [42] using zero-initialized convolution layer to inject 2D human pose condition. Addressing the challenge caused by sparse pose conditions, PoCoLD [17] adopts DensePose [16] as a robust pose representation. Meanwhile, pose-guided person video generation is also noticeable. Recent works such as DreamPose [28] and AnimateAnyone [23] generate a video guided by pose-sequence which is temporally coherent, and use the fine-tuning method. MagicAnimate [56] also generates a video guided by pose-sequence conditions, but leverages pose ControlNet [61] as a pose injector. Champ [75], a subsequent work of AnimateAnyone [23] and MagicAnimate [56], uses SMPL [36] guidance instead of only 2D human pose.

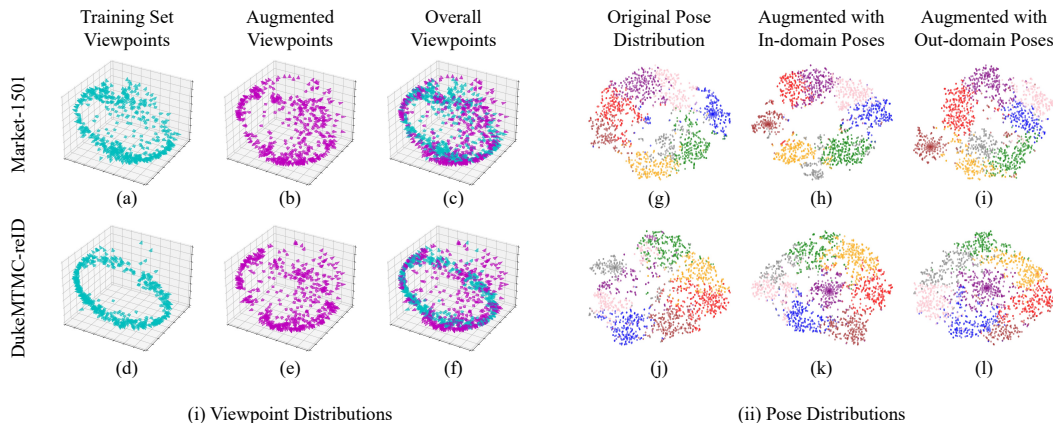


Figure 3: **Visualization of the effect of viewpoint and human pose augmentation.** We compare visualizations of camera viewpoint and human pose distributions for the Market-1501 [65] and DukeMTMC-reID datasets [71]. The left figures (i) display the camera viewpoint distribution derived from SMPL [35], while the right figures (ii) illustrate the pose distribution. In (i), from left to right, we show the viewpoint distributions of the training dataset, the augmented dataset, and the combination of both. Similarly, in (ii), from left to right, we present t-SNE [50] visualizations of the human pose distributions, showing poses from the training dataset, poses used for augmentation, and the combination of both. These visualizations demonstrate that our pose augmentation successfully diversifies both viewpoint and human pose distributions.

3 Method

3.1 Motivation and Overview

In this paper, we tackle the challenging Re-ID problem of *limited camera viewpoints and human poses in training datasets*. Re-ID datasets typically contain a limited number of cameras, ranging from 6 in Market-1501 [65] to 8 in the DukeMTMC-reID dataset [71]. This small number of fixed cameras capture individuals within a restricted range of viewpoints, significantly impacting the generalization performance of Re-ID models. Furthermore, since the cameras mostly capture people walking or standing still, this also affects the generalization capabilities of Re-ID models. The analysis in Figure 2 illustrates the restricted camera viewpoints and human poses captured in the training dataset.

We aim to diversify the range of camera viewpoints and human poses by augmenting the training dataset with generative models. However, generative models sample from the training dataset distribution. Without explicit consideration for generalization, the quality of generated images with camera viewpoints and human poses that are rarely present in the training dataset distribution may be compromised. To address this, we leverage the powerful generalization capability of a foundation generative model trained on a billion-scale dataset, *i.e.*, Stable Diffusion [42]. We carefully select and integrate components to enable camera viewpoint and human pose conditioning within the generative model for augmentation. By leveraging its generalization ability and applying viewpoint conditioning, we can effectively augment the training dataset with diverse camera viewpoints and human poses, as shown in Figure 3.

In this section, we explain the augmentation process in Sec. 3.2. Subsequently, we present human pose and camera viewpoint condition from SMPL in Sec. 3.3, and how to inject condition with identity into diffusion model in Sec. 3.4.

3.2 Pose-Diversified Augmentation with Diffusion Models

To mitigate the biased camera viewpoint and human pose in training dataset, we augment images with *uniformly distributed camera viewpoint and human poses sourced from outside the training dataset*. Specifically, for camera viewpoints, we augment the images adjusting two factor: elevation and azimuth. For the elevation, we uniformly sample from 0° to 30° , assuming that the camera is not positioned below the ground and that a person becomes indistinguishable when the camera is

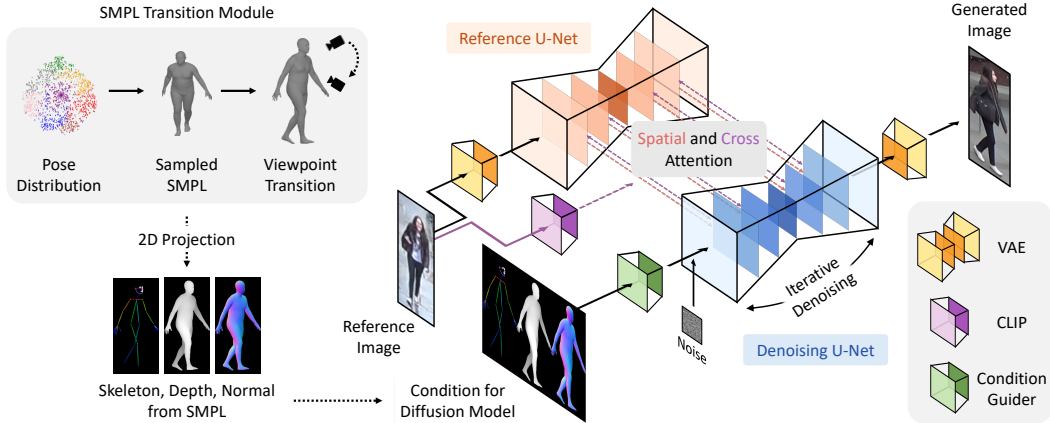


Figure 4: **Overall architecture of Diff-ID.** Given the viewpoint and pose distributions, we first render the body shape sampled from the distribution using SMPL [36], generating the corresponding skeleton, depth map, and normal maps. These conditions, along with a reference image for identity preservation, are then fed into Diff-ID, which consists of two branches: the reference U-Net processes the identity information from the reference image, while the denoising U-Net generates a person with the same identity, given the input conditions. The denoising U-Net generates images by iterating through the denoising process.

positioned above a certain degree. For the azimuth, we randomly sample from 0° to 360° , as a person can be captured in any random direction. With these consideration, we found the distribution of camera viewpoint is significantly unbiased, as depicted in Figure 2. For human poses, we source them from outside the training dataset for diversification, e.g., using poses extracted from dance videos [4]. This significantly diversifies the human poses, facilitating generalization to various poses during testing. Given predefined camera and pose distributions sourced from outside the training dataset, we aim to augment the training dataset using a generative model conditioned on the camera and pose.

3.3 Human Pose and Camera Viewpoint Condition from SMPL

To augment the data with varying human pose and camera viewpoint, we provide specific conditions to the diffusion model. Previous works [11, 40, 49] have primarily addressed pose control by providing a human pose skeleton. However, relying solely on the human skeleton has limitations due to missing information: When projected onto 2D images, the human skeleton lacks depth information, posing ambiguity for the model when inferring viewpoint information from the skeleton. For example, if the camera is above a person, the skeleton would appear compressed vertically. Without depth information, the model cannot distinguish whether the camera is positioned above the person or the person is simply short.

In this regard, in addition to the human pose skeleton, we utilize SMPL [36], a human body model used for realistic human rendering. SMPL [36] can model intricate human shapes, including complex body articulations in 3D space. From this human model, we can easily extract 2D representations of the 3D human by rendering the model, such as depth maps which implicitly contain camera viewpoint information.

To provide rich information about camera viewpoint, we use depth maps from SMPL [36] as a condition for the diffusion model, along with the human skeleton and a photo to control identity. Additionally, we incorporate surface normals from SMPL [36], as they encode detailed human surface information and can help generate more precise augmentations. Gathering these conditions, we feed them to diffusion model as a guidance.

The conditions can be classified into two categories: 1) Conditions that should be spatially aligned with the generated output, such as depth information from SMPL [36] and the human skeleton. 2) Conditions that are not necessarily spatially aligned with the generated output, such as identity information. While maintaining the original U-Net [43] structure to preserve its pre-trained knowledge, we carefully add components to the Stable Diffusion model to handle these two different types of conditions.

3.4 Conditional Diffusion Models for Pose-Diversified Augmentation

To generate images with diverse camera viewpoints and human poses, we specifically design a model conditioned on such information. However, when training the generative model on a human Re-ID dataset without careful consideration, it may produce degenerated results for camera viewpoints or human poses that are rarely present in the training dataset.

In this work, we address this problem by leveraging the vast knowledge in pre-trained Stable Diffusion [42]. We first provide a preliminary explanation of the Stable Diffusion model [42], followed by how to augment images in the training dataset while controlling their human pose, camera viewpoint, and identity. The overall architecture can be seen in Figure 4.

Preliminary: Stable Diffusion model. Diffusion model [21, 42, 48] is a generative model that samples images from the learned data distribution $p(x)$ through iterative denoising process from Gaussian noise. Our method builds upon Stable Diffusion (SD) [42]. SD performs a denoising process in a latent space of Autoencoder [59], reducing the computational cost compared to denoising in the pixel space [21, 48]. Specifically, the encoder in SD maps a given image \mathbf{x} into a latent representation \mathbf{z} , denoted as $\mathbf{z} = \mathcal{E}(\mathbf{x})$.

In training time, SD learns a denoising U-Net [43] ϵ_θ that predict normally distributed noise ϵ given a noised latent \mathbf{z}_t , which is a noisy latent of \mathbf{z} with a Gaussian noise at noise level t . This U-Net function can be trained with a following objective:

$$\mathcal{L} = \mathbb{E}_{\mathbf{z}_t, c, \epsilon, t} (\|\epsilon - \epsilon_\theta(\mathbf{z}_t, c, t)\|_2^2), \quad (1)$$

where c denotes conditional information for generation. The condition, provided by a text description, is encoded using the CLIP text encoder [41], enabling controllability over the image generation process. The denoising U-Net is composed of three parts: downsampling block, bottleneck block, and upsampling block. Each block consists of a combination of 2D convolutional layers, self-attention layers, and cross-attention layers.

During inference, a sample \mathbf{z}_T from a Gaussian distribution is gradually denoised using the trained denoising U-Net. Undergoing the denoising process from $t = T$ to $t = 0$, the model generates \mathbf{z}_0 . This final latent representation is then passed through the decoder \mathcal{D} to produce the output image.

Injecting human pose and camera viewpoint into diffusion model. For conditions that should be spatially aligned with the generated output, we process them with a respective pose guider network and concatenate the processed conditions along the channel dimension. Specifically, the depth map $\mathbf{d} \in \mathbb{R}^{H \times W \times 1}$, surface normals $\mathbf{n} \in \mathbb{R}^{H \times W \times 3}$, and rendered human skeleton $\mathbf{s} \in \mathbb{R}^{H \times W \times 3}$ are each processed by a respective pose guider network. This network reduces the spatial size of the condition to $1/8$ of the original size and embeds the pose information into $\mathbb{R}^{\frac{H}{8} \times \frac{W}{8} \times C}$ embeddings, aligning it with the size of the latent representation in the diffusion model. The last layer of the pose guider network is initialized to zeros to minimize the initial degradation during the fine-tuning stage of the pre-trained SD model. The processed conditions are then concatenated along the channel dimension and added to the projected noise before it is fed into the U-Net.

Injecting identity into diffusion model as a condition. For human identity, unlike the condition that is spatially aligned with the output, it is not necessarily aligned with the output. In this regard, instead of adding the condition pixel-wise, we provide the identity information to the denoising U-Net with attention. Specifically, we design a reference U-Net that has the same architecture as the denoising U-Net, while the weights of the U-Net are initialized with a pre-trained Stable Diffusion model. To inject the identity of an image into the denoising U-Net, we first feed the image into the reference U-Net. Then, the identity information is shared with the denoising U-Net using self-attention for each block. In more detail, given the intermediate feature map from the denoising U-Net $f_1 \in \mathbb{R}^{(h \times w) \times c}$ and from the reference U-Net $f_2 \in \mathbb{R}^{(h \times w) \times c}$, they are concatenated along the spatial dimension, followed by the self-attention layer. Then, the first half of the output is used as the input for the following layers in the denoising U-Net. In this way, the two parallel branches can benefit from the extensive pre-trained knowledge of Stable Diffusion. Additionally, the identical architecture of the two branches facilitates training by sharing the same feature space. For the cross-attention part in Stable Diffusion where text embeddings from CLIP are used, we instead utilize image embeddings from the CLIP image encoder. This is possible because both text and image embeddings are trained to reside in the same embedding space.

4 Experiments

4.1 Implementation Details

We utilize ResNet50 [18] as the feature backbone for our Re-ID model, initialized with weights pre-trained on ImageNet1K [44]. The training of our generative model is conducted in two stages: initially learning a general human representation using a fashion video dataset [60], followed by fine-tuning the model with person Re-ID datasets. Throughout both stages, the weights of the autoencoders [59] and CLIP [41] image encoder are frozen, focusing on the reference U-Net, denoising U-Net, and pose guider.

In the first stage, the reference U-Net and denoising U-Net are initialized from the original Stable Diffusion [42] model and fine-tuned with the fashion video dataset [60]. The fashion video dataset [60], comprising 192,402 frames from 500 human videos. All input images are resized to 768×768 with a batch size of 2. Mean Squared Error (MSE) loss is calculated for each pair of a generated images, optimized using Adam [29] with a learning rate of $1e-5$ and weight decay of 0.01. Training for 30,000 iterations takes 15 hours on one NVIDIA RTX A6000 GPU.

In the second stage, the generative model pre-trained on the fashion video dataset [60] is fine-tuned with Re-ID datasets consisting of pedestrian images from CCTV cameras. Images are resized to 192×384 , we increased the batch size to 4. The training process is the same as in the previous stage. It takes about 6-7 hours for the DukeMTMC-reID [71] dataset with 16,522 training images and the Market1501 [65] dataset with 12,936 training images on one NVIDIA RTX A6000 GPU.

Our work employs data augmentation via a generative model to enrich the training data for the Re-ID model. We start by randomly sampling 20 target pose guidances from the Everybody Dance Now dataset [4], an out-of-domain dataset not used in the training of the Re-ID model. Next, we randomly sample between 5 to 7 instances from each frame sequence of person identity (pid) in Re-ID datasets and input these instances into the generative model. The generative model then produces 65 to 70 images for each sampled instance, resulting in an generated dataset. From this generated dataset, which consists of 80,000 images, we randomly sample approximately 45,500 and 49,000 images for Market-1501 and DukeMTMC-reID, respectively. These generated images are then added to the original training datasets to create the augmented training sets. For the DukeMTMC-reID [71] dataset, which originally consists of 16,522 training images from 702 pids, the addition of approximately 49,000 generated images results in a new training set comprising 30,522 images from 702 pids. Similarly, for the Market-1501 [65] dataset, which originally consists of 12,936 training images from 750 pids, the addition of approximately 45,500 generated images results in a new training set comprising 26,936 images from 750 pids. This augmentation strategy leverages the generative model to significantly increase the diversity and quantity of the training data, thereby enhancing the model’s ability to generalize and perform effectively on the Person Re-identification task.

4.2 Experimental Details

We perform experiments on two publicly available person Re-ID datasets, *i.e.*, Market-1501 [65] and DukeMTMC-reID [71]. We present results using two standard Re-ID metrics: cumulative matching characteristics at Rank-1 (R1) and mean average precision (mAP).

We trained our Re-ID model with augmented Re-ID datasets: Market-1501 [65] and DukeMTMC-reID [71]. For each training iteration, the batch size of pids is set to 32 and the number of instances per pid is set to 8, resulting in a total batch size of 256. We utilize Triplet loss [22] and classification loss to distinguish different person identities. The triplet loss [22] is calculated by first obtaining the euclidean distance between each instance using the 2,048-dimensional feature extracted from ResNet50 [18]. The objective is to ensure that the hard-negative distance, the shortest distance between instances of different person identities, is larger than the hard-positive distance, the longest distance between instances of the same person identity. The margin of the triplet loss [22] is set to 0.5, meaning the gap between the hard-negative distance and the hard-positive distance should be larger than 0.5. In addition to the triplet loss [22], we use a classification loss, which is a CrossEntropy [62] loss computed between the pid and the output logits from the classifier. The total loss for training is the sum of the triplet loss and the classification loss. We apply the Adam [29] optimizer with different learning rates for ResNet50 [18] and the classifier. For the ResNet50 [18] backbone, we set

Table 1: **Quantitative validation of our design choices.**

	Diverse Human Pose Augmentation	Diverse Viewpoint Augmentation	Pre-trained Diffusion	Market-1501			DukeMTMC		
				mAP	R1	R5	mAP	R1	R5
(I)	✗	✗	✗	68.5	84.9	92.4	55.5	73.6	85.4
(II)	✗	✗	✓	68.6	85.0	92.5	55.8	73.4	85.2
(III)	✗	✓	✓	69.5	86.2	93.9	60.5	77.4	87.2
(IV)	✓	✗	✓	69.4	86.1	93.6	60.1	77.2	86.9
(V)	✓	✓	✗	67.6	84.5	93.4	54.1	72.2	83.8
(VI)	✓	✓	✓	72.6	87.4	94.5	63.2	78.7	88.5

Table 2: **Quantitative comparison of different settings.** We gradually increase the ratio of generated images and compare the results of various settings. Each row represents the result for an approximate number of augmented images.

# of Images	Market-1501		DukeMTMC	
	mAP	R1	mAP	R1
3,500	69.8	86.4	57.3	75.0
7,000	71.1	86.3	60.0	76.5
10,500	71.6	87.0	61.2	77.2
14,000	71.1	86.4	61.2	77.6
17,500	71.5	86.2	62.1	77.2
21,000	71.5	86.0	62.5	78.3
24,500	72.1	86.6	62.5	77.5
28,000	72.0	86.7	62.2	77.8
31,500	72.2	87.0	62.3	77.7
35,000	72.2	87.2	62.1	77.8
38,500	72.2	86.8	62.4	77.3
42,000	72.1	86.9	62.6	78.1
45,500	72.6	87.4	62.8	77.6
49,000	72.4	86.6	63.2	78.7
52,500	72.4	87.0	62.9	78.1
56,000	72.4	86.7	62.4	77.6

the learning rate to 1e-5, and for the classifier, we set the learning rate to 1e-4. The training process with 20,000 iterations takes approximately 2 hours on two NVIDIA RTX A6000 GPUs.

4.3 Ablation Study and Analysis

In Table 1, we conduct an ablation study to verify our design choices: 1) human pose augmentation, 2) camera viewpoint augmentation, and 3) the effectiveness of the pre-trained diffusion model.

(I) is a baseline Re-ID model trained on the original dataset, where Diff-ID is not used for the augmentation. For (II), we train a diffusion model on the training dataset and augment the data using random human poses and viewpoints within the training distribution. The marginal performance gain from (I) to (II) demonstrates that augmentation within the training distribution is insufficient. For (III) and (IV), we augment the training dataset using diverse human poses from an external dataset and uniformly sampled viewpoints, respectively. Both augmentations show significant performance gains. Notably, for the DukeMTMC-reID dataset [71], which exhibits a stronger bias in camera viewpoints, we observe improvements of 4.7%p and 4.3%p for each augmentation strategy. This validates the effectiveness of targeting the biased distributions of human pose and viewpoint for augmentation. In (V), we use the same architecture as Diff-ID, except for the initialization, where we randomly initialize the SD model instead of using its pre-trained weights. We found that with random initialization, the performance is even worse than the baseline (I). We believe this is because a diffusion model trained from scratch has limited ability to generalize to poses or viewpoints rarely seen in the training set. This result supports our decision to leverage the pre-trained knowledge of SD. (VI) demonstrates the final version of our model. The performance gains from both (III) and (IV) prove that both types of augmentation are useful and have a complementary effect, leading to further performance improvements.

Table 3: **Quantitative comparison on standard Re-ID benchmarks.** Note that the Re-ID Experts in the first row group are not directly comparable, as our primary focus is on *dataset generation*. For augmentation-based methods, we train the same Re-ID model on the datasets generated by each method to ensure a fair comparison. *: The authors did not provide a pre-trained model.

Methods	Market-1501		DukeMTMC	
	mAP	R1	mAP	R1
<i>Re-ID Experts</i>				
LTReID [52]	89.0	95.9	80.4	90.5
DRL-Net [25]	86.9	94.7	76.6	88.1
BPB-ReID [47]	89.4	95.7	84.2	92.4
AAformer [74]	87.7	95.4	80.0	90.1
CLIP-ReID [31]	90.5	95.4	83.1	90.8
<i>Augmentation-based Methods</i>				
FD-GAN [12]	68.1	85.1	51.3	69.3
Xing-GAN [49]	70.3	86.1	-*	-*
Diff-ID (Ours)	72.6	87.4	63.2	78.7



Figure 5: **Qualitative comparison.** We qualitatively compare the generated output to FD-GAN [11] and XingGAN [49]. Our method demonstrates significantly better fidelity while faithfully capturing the identity of the person in the reference image and accurately following the target pose.

In Table 2, we present an additional ablation study to determine the optimal number of images used in augmentation. The proposed settings aim to evaluate the effect of increasing the training dataset size. We randomly sample between 5 to 7 instances from each frame sequence of person identity (pid) in the Re-ID datasets and input these instances into the generative model. The generative model produces a minimum of 5 to a maximum of 80 images for each sampled instance. We then incorporate varying numbers of these generated images to the original dataset.

We expected to see higher results as the size of the augmented dataset increased. However, in both cases using different datasets, namely the DukeMTMC-reID dataset [71] and Market-1501 [65], there is an optimal number of images that enhance performance. For Market-1501 dataset, the highest result is obtained when approximately 45,500 images are added. For DukeMTMC-reID dataset, the highest result is obtained when approximately 49,000 images are added. This result demonstrates the high quality of the generated images, as adding a significant number of images still results in high performance.

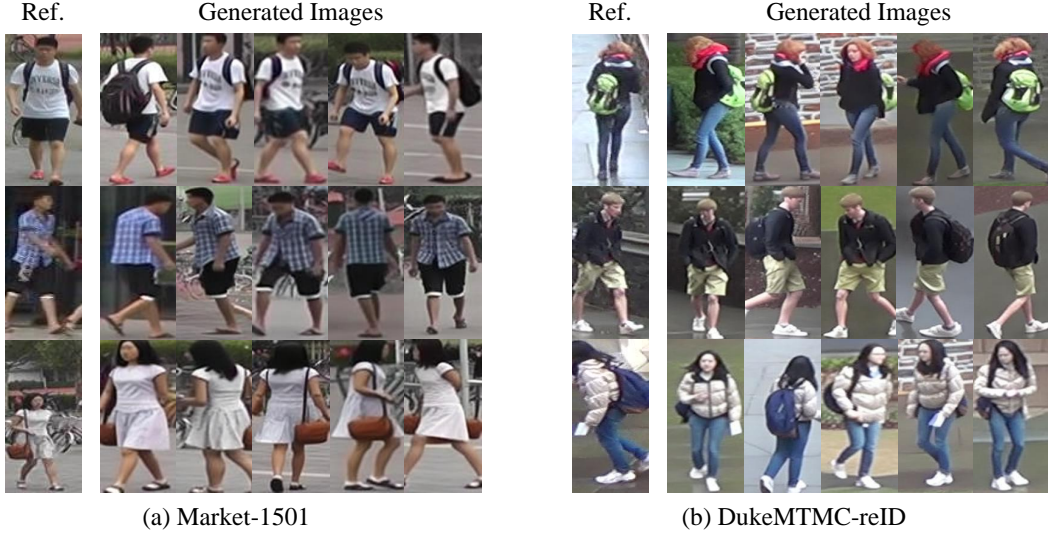


Figure 6: **Visualization of generated data.** Given a reference image, we sample five images generated by our method. These outputs demonstrate the model’s capability to produce diverse and realistic variations. Ref. denotes the reference image.



Figure 7: **Generated results under comprehensive conditions.** Using a reference image of individuals carrying backpacks, we generate back views using our method. This demonstrates that our method can be effectively applied under complex and potentially confusing conditions.

4.4 Quantitative Comparisons

In this section, we evaluate the performance of our method, and compare it with the augmentation-based Re-ID methods. The results are shown in Table 3. Note that our augmentation method can be applied to arbitrary Re-ID models, and the performance can be improved when better Re-ID method is applied.

To ensure a fair assessment and maintain consistency, the same Re-ID model architecture was used to train on datasets produced by each augmentation method. Compared to previous augmentation methods, our augmentation method demonstrates significantly improved performance. This result also validates our augmentation framework, highlighting the effectiveness of filling in the sparsely distributed poses and viewpoints. Note that the first row group, Re-ID Experts, is not directly comparable to our methods, as our primary focus is on addressing biases in the training dataset rather than developing superior Re-ID models.

4.5 Qualitative Results

In Figure 5, we present a qualitative comparison to GAN-based augmentation methods [33, 69, 70]. Unlike GAN-based methods, Diff-ID effectively generates poses sourced from outside the dataset.

GAN-based methods struggle to generalize to diverse poses, resulting in blurry outputs and a limited ability to maintain the identity of the reference and the target pose, especially when dealing with complex elements like accessories or specific clothing details. This issue is particularly pronounced when generating images of people carrying bags. GAN-based methods often fail to accurately distinguish between bag and the person’s clothing, leading to confusion. For example, they might generate person’s top in the color of the bag from the reference image, or alter the shape and color of the bag, or even change the entire outfit based on the bag’s color, as shown in Figure 5. This confusion is especially prevalent when the reference image features a backpack, which can cover the person’s entire back in the back view, making it easily mistaken for a top. This is due to GAN-based models’ lack of general knowledge about the world.

In contrast, large-scale generative models possess comprehensive knowledge about humans, their clothing, and accessories. They understand the context of outfits and generate images that preserve the identity of the reference image. This advantage underscores our decision to utilize a large-scale pre-trained diffusion model, which can generalize to poses and viewpoints underrepresented in the training dataset. Its extensive pre-training on a diverse range of data enables it to handle these complexities more effectively.

4.6 Visualization of Generated Data

In Figure 6, we present visualization results on two datasets, DukeMTMC-reID [71] and Market-1501 [65]. Given a reference image, our method faithfully preserves its identity while being able to generate diverse poses with high fidelity.

Given a reference image, our method leverages the strengths of a large-scale pre-trained diffusion model to maintain the intricate details of the subject’s identity. This includes preserving clothing details, and other distinguishing characteristics, ensuring that the generated images are not only visually coherent but also identity-consistent with the reference image.

In the DukeMTMC-reID [71] and Market-1501 [65] dataset, our method excels in generating various poses while preserving the unique identities of the individuals. Our method demonstrates its capability to generate high-fidelity images that faithfully reproduce the identities of the reference subjects across a range of poses and viewpoints.

Furthermore, our approach, facilitated by the large-scale pre-trained diffusion model, showcases an enhanced understanding of contextual details, such as the interaction between the person and their clothing or accessories by facilitate large-scale pre-trained diffusion model. This allows our model to generate more realistic and contextually accurate images. For instance, when the reference image includes a person carrying a bag, our model accurately distinguishes between the bag and the person’s clothing, ensuring that both elements are rendered correctly in the generated images. More qualitative results about this is shown in Figure 7.

For the additional qualitative results, please refer to Appendix A.

5 Conclusion

In this paper, we proposed **Diff-ID**, a novel data augmentation approach that leverages pre-trained diffusion models to diversify pose and viewpoint distributions in person re-identification training datasets. By sampling from outside pose sources and uniformly distributed camera viewpoints, we augmented Re-ID datasets with realistic images of individuals in rare poses and from uncommon camera angles. This augmentation strategy enables the training of Re-ID models that are more robust to variations in human pose and camera viewpoint. The key to Diff-ID’s success lies in its ability to integrate pose, viewpoint, and identity conditions into large-scale pre-trained diffusion models like Stable Diffusion [42], effectively leveraging the vast knowledge embedded in these models for generating high-quality augmented data. Comprehensive experiments on the Market-1501 [65] and DukeMTMC-reID [71] benchmarks demonstrated the effectiveness of our approach, with Diff-ID achieving significant performance improvements compared to baselines without data augmentation. Ablation studies further verified the importance of both diverse pose augmentation and camera viewpoint augmentation in enhancing the generalization capabilities of Re-ID models.

References

- [1] Slawomir Bak, Sofia Zaidenberg, Bernard Boulay, and François Bremond. Improving person re-identification by viewpoint cues. In *2014 11th IEEE International Conference on Advanced Video and Signal Based Surveillance (AVSS)*, pages 175–180. IEEE, 2014.
- [2] Ankan Kumar Bhunia, Salman Khan, Hisham Cholakkal, Rao Muhammad Anwer, Jorma Laaksonen, Mubarak Shah, and Fahad Shahbaz Khan. Person image synthesis via denoising diffusion model. In *Proceedings of the IEEE/CVF Conference on Computer Vision and Pattern Recognition*, pages 5968–5976, 2023.
- [3] Zhe Cao, Tomas Simon, Shih-En Wei, and Yaser Sheikh. Realtime multi-person 2d pose estimation using part affinity fields. In *Proceedings of the IEEE conference on computer vision and pattern recognition*, pages 7291–7299, 2017.
- [4] Caroline Chan, Shiry Ginosar, Tinghui Zhou, and Alexei A Efros. Everybody dance now. In *Proceedings of the IEEE/CVF international conference on computer vision*, pages 5933–5942, 2019.
- [5] Weihua Chen, Xianzhe Xu, Jian Jia, Hao Luo, Yaohua Wang, Fan Wang, Rong Jin, and Xiuyu Sun. Beyond appearance: a semantic controllable self-supervised learning framework for human-centric visual tasks. In *Proceedings of the IEEE/CVF Conference on Computer Vision and Pattern Recognition*, pages 15050–15061, 2023.
- [6] Ying-Cong Chen, Xiatian Zhu, Wei-Shi Zheng, and Jian-Huang Lai. Person re-identification by camera correlation aware feature augmentation. *IEEE TRANSACTIONS ON PATTERN ANALYSIS AND MACHINE INTELLIGENCE*, 40(2), 2018.
- [7] Yeong-Jun Cho and Kuk-Jin Yoon. Improving person re-identification via pose-aware multi-shot matching. In *2016 IEEE Conference on Computer Vision and Pattern Recognition, CVPR 2016*, pages 1354–1362. IEEE Computer Society and the Computer Vision Foundation (CVF), 2016.
- [8] Serhan Coşar and Nicola Bellotto. Human re-identification with a robot thermal camera using entropy-based sampling. *Journal of Intelligent & Robotic Systems*, 98(1):85–102, 2020.
- [9] Zuozhuo Dai, Mingqiang Chen, Xiaodong Gu, Siyu Zhu, and Ping Tan. Batch dropblock network for person re-identification and beyond. In *2019 IEEE/CVF International Conference on Computer Vision (ICCV)*, pages 3690–3700. IEEE Computer Society, 2019.
- [10] Dengpan Fu, Dongdong Chen, Jianmin Bao, Hao Yang, Lu Yuan, Lei Zhang, Houqiang Li, and Dong Chen. Unsupervised pre-training for person re-identification. In *Proceedings of the IEEE/CVF conference on computer vision and pattern recognition*, pages 14750–14759, 2021.
- [11] Yixiao Ge, Zhuowan Li, Haiyu Zhao, Guojun Yin, Shuai Yi, Xiaogang Wang, et al. Fd-gan: Pose-guided feature distilling gan for robust person re-identification. *Advances in neural information processing systems*, 31, 2018.
- [12] Yixiao Ge, Zhuowan Li, Haiyu Zhao, Guojun Yin, Shuai Yi, Xiaogang Wang, and Hongsheng Li. Fd-gan: Pose-guided feature distilling gan for robust person re-identification. In *Advances in Neural Information Processing Systems*, pages 1229–1240, 2018.
- [13] Yunpeng Gong, Liqing Huang, and Lifei Chen. Eliminate deviation with deviation for data augmentation and a general multi-modal data learning method. *arXiv preprint arXiv:2101.08533*, 2021.
- [14] Yunpeng Gong, Liqing Huang, and Lifei Chen. Eliminate deviation with deviation for data augmentation and a general multi-modal data learning method. *arXiv preprint arXiv:2101.08533*, 2021.
- [15] Ian Goodfellow, Jean Pouget-Abadie, Mehdi Mirza, Bing Xu, David Warde-Farley, Sherjil Ozair, Aaron Courville, and Yoshua Bengio. Generative adversarial networks. *Communications of the ACM*, 63(11):139–144, 2020.
- [16] Rıza Alp Güler, Natalia Neverova, and Iasonas Kokkinos. Densepose: Dense human pose estimation in the wild. In *Proceedings of the IEEE conference on computer vision and pattern recognition*, pages 7297–7306, 2018.
- [17] Xiao Han, Xiatian Zhu, Jiankang Deng, Yi-Zhe Song, and Tao Xiang. Controllable person image synthesis with pose-constrained latent diffusion. In *Proceedings of the IEEE/CVF International Conference on Computer Vision*, pages 22768–22777, 2023.

- [18] Kaiming He, Xiangyu Zhang, Shaoqing Ren, and Jian Sun. Deep residual learning for image recognition. In *Proceedings of the IEEE conference on computer vision and pattern recognition*, pages 770–778, 2016.
- [19] Tianyu He, Xin Jin, Xu Shen, Jianqiang Huang, Zhibo Chen, and Xian-Sheng Hua. Dense interaction learning for video-based person re-identification. In *Proceedings of the IEEE/CVF International Conference on Computer Vision*, pages 1490–1501, 2021.
- [20] Martin Hirzer, Peter M Roth, Martin Köstinger, and Horst Bischof. Relaxed pairwise learned metric for person re-identification. In *Computer Vision–ECCV 2012: 12th European Conference on Computer Vision, Florence, Italy, October 7–13, 2012, Proceedings, Part VI 12*, pages 780–793. Springer, 2012.
- [21] Jonathan Ho, Ajay Jain, and Pieter Abbeel. Denoising diffusion probabilistic models. *Advances in neural information processing systems*, 33:6840–6851, 2020.
- [22] Elad Hoffer and Nir Ailon. Deep metric learning using triplet network. In *Similarity-Based Pattern Recognition: Third International Workshop, SIMBAD 2015, Copenhagen, Denmark, October 12–14, 2015. Proceedings 3*, pages 84–92. Springer, 2015.
- [23] Li Hu, Xin Gao, Peng Zhang, Ke Sun, Bang Zhang, and Liefeng Bo. Animate anyone: Consistent and controllable image-to-video synthesis for character animation. *arXiv preprint arXiv:2311.17117*, 2023.
- [24] Houjing Huang, Dangwei Li, Zhang Zhang, Xiaotang Chen, and Kaiqi Huang. Adversarially occluded samples for person re-identification. In *2018 IEEE/CVF Conference on Computer Vision and Pattern Recognition (CVPR)*, pages 5098–5107. IEEE Computer Society, 2018.
- [25] Mengxi Jia, Xinhua Cheng, Shijian Lu, and Jian Zhang. Learning disentangled representation implicitly via transformer for occluded person re-identification. *IEEE Transactions on Multimedia*, 25:1294–1305, 2022.
- [26] Siddhant Kapil. Locally aware transformer for person re-identification. Master’s thesis, University of Maryland, Baltimore County, 2021.
- [27] Srikrishna Karanam, Yang Li, and Richard J Radke. Person re-identification with discriminatively trained viewpoint invariant dictionaries. In *2015 IEEE International Conference on Computer Vision (ICCV)*, pages 4516–4524. IEEE, 2015.
- [28] Johanna Karras, Aleksander Holynski, Ting-Chun Wang, and Ira Kemelmacher-Shlizerman. Dreampose: Fashion image-to-video synthesis via stable diffusion. In *2023 IEEE/CVF International Conference on Computer Vision (ICCV)*, pages 22623–22633. IEEE, 2023.
- [29] Diederik P Kingma and Jimmy Ba. Adam: A method for stochastic optimization. *arXiv preprint arXiv:1412.6980*, 2014.
- [30] Martin Koestinger, Martin Hirzer, Paul Wohlhart, Peter M Roth, and Horst Bischof. Large scale metric learning from equivalence constraints. In *2012 IEEE conference on computer vision and pattern recognition*, pages 2288–2295. IEEE, 2012.
- [31] Siyuan Li, Li Sun, and Qingli Li. Clip-reid: exploiting vision-language model for image re-identification without concrete text labels. In *Proceedings of the AAAI Conference on Artificial Intelligence*, volume 37, pages 1405–1413, 2023.
- [32] Shengcai Liao and Stan Z Li. Efficient psd constrained asymmetric metric learning for person re-identification. In *Proceedings of the IEEE international conference on computer vision*, pages 3685–3693, 2015.
- [33] Jinxian Liu, Bingbing Ni, Yichao Yan, Peng Zhou, Shuo Cheng, and Jianguo Hu. Pose transferrable person re-identification. In *2018 IEEE/CVF Conference on Computer Vision and Pattern Recognition*. IEEE, 2018.
- [34] Xiao Liu, Mingli Song, Dacheng Tao, Xingchen Zhou, Chun Chen, and Jiajun Bu. Semi-supervised coupled dictionary learning for person re-identification. In *2014 IEEE Conference on Computer Vision and Pattern Recognition (CVPR)*, pages 3550–3557. IEEE Computer Society, 2014.
- [35] Matthew Loper, Naureen Mahmood, Javier Romero, Gerard Pons-Moll, and Michael J Black. Smpl: A skinned multi-person linear model. *Acm Transactions on Graphics*, 34(Article 248), 2015.

- [36] Matthew Loper, Naureen Mahmood, Javier Romero, Gerard Pons-Moll, and Michael J Black. Smpl: A skinned multi-person linear model. In *Seminal Graphics Papers: Pushing the Boundaries, Volume 2*, pages 851–866. 2023.
- [37] Chuanchen Luo, Chunfeng Song, and Zhaoxiang Zhang. Generalizing person re-identification by camera-aware invariance learning and cross-domain mixup. In *Computer Vision–ECCV 2020: 16th European Conference, Glasgow, UK, August 23–28, 2020, Proceedings, Part XV 16*, pages 224–241. Springer, 2020.
- [38] H Luo, W Jiang, Y Gu, F Liu, X Liao, S Lai, and J Gu. A strong baseline and batch normneuralization neck for deep person reidentification. *arXiv preprint arXiv:1906.08332*, 2019.
- [39] Niall McLaughlin, Jesus Martinez Del Rincon, and Paul Miller. Data-augmentation for reducing dataset bias in person re-identification. In *2015 12th IEEE International Conference on Advanced Video and Signal Based Surveillance (AVSS)*, pages 1–6. IEEE Computer Society, 2015.
- [40] Xuelin Qian, Yanwei Fu, Tao Xiang, Wenxuan Wang, Jie Qiu, Yang Wu, Yu-Gang Jiang, and Xiangyang Xue. Pose-normalized image generation for person re-identification. In *Proceedings of the European conference on computer vision (ECCV)*, pages 650–667, 2018.
- [41] Alec Radford, Jong Wook Kim, Chris Hallacy, Aditya Ramesh, Gabriel Goh, Sandhini Agarwal, Girish Sastry, Amanda Askell, Pamela Mishkin, Jack Clark, et al. Learning transferable visual models from natural language supervision. In *International conference on machine learning*, pages 8748–8763. PMLR, 2021.
- [42] Robin Rombach, Andreas Blattmann, Dominik Lorenz, Patrick Esser, and Björn Ommer. High-resolution image synthesis with latent diffusion models. In *Proceedings of the IEEE/CVF conference on computer vision and pattern recognition*, pages 10684–10695, 2022.
- [43] Olaf Ronneberger, Philipp Fischer, and Thomas Brox. U-net: Convolutional networks for biomedical image segmentation. In *Medical image computing and computer-assisted intervention–MICCAI 2015: 18th international conference, Munich, Germany, October 5-9, 2015, proceedings, part III 18*, pages 234–241. Springer, 2015.
- [44] Olga Russakovsky, Jia Deng, Hao Su, Jonathan Krause, Sanjeev Satheesh, Sean Ma, Zhiheng Huang, Andrej Karpathy, Aditya Khosla, Michael Bernstein, et al. Imagenet large scale visual recognition challenge. *International journal of computer vision*, 115:211–252, 2015.
- [45] M Saquib Sarfraz, Arne Schumann, Andreas Eberle, and Rainer Stiefelhagen. A pose-sensitive embedding for person re-identification with expanded cross neighborhood re-ranking. In *Proceedings of the IEEE conference on computer vision and pattern recognition*, pages 420–429, 2018.
- [46] Vladimir Somers, Christophe De Vleeschouwer, and Alexandre Alahi. Body part-based representation learning for occluded person re-identification. In *Proceedings of the IEEE/CVF Winter Conference on Applications of Computer Vision (WACV)*, pages 1613–1623, January 2023.
- [47] Vladimir Somers, Christophe De Vleeschouwer, and Alexandre Alahi. Body part-based representation learning for occluded person re-identification. In *Proceedings of the IEEE/CVF winter conference on applications of computer vision*, pages 1613–1623, 2023.
- [48] Jiaming Song, Chenlin Meng, and Stefano Ermon. Denoising diffusion implicit models. *arXiv preprint arXiv:2010.02502*, 2020.
- [49] Hao Tang, Song Bai, Li Zhang, Philip HS Torr, and Nicu Sebe. Xingan for person image generation. In *Computer Vision–ECCV 2020: 16th European Conference, Glasgow, UK, August 23–28, 2020, Proceedings, Part XXV 16*, pages 717–734. Springer, 2020.
- [50] Laurens Van der Maaten and Geoffrey Hinton. Visualizing data using t-sne. *Journal of machine learning research*, 9(11), 2008.
- [51] Guangcong Wang, Jianhuang Lai, Peigen Huang, and Xiaohua Xie. Spatial-temporal person re-identification. In *Proceedings of the AAAI conference on artificial intelligence*, volume 33, pages 8933–8940, 2019.
- [52] Pingyu Wang, Zhicheng Zhao, Fei Su, and Hongying Meng. Lt Reid: Factorizable feature generation with independent components for long-tailed person re-identification. *IEEE Transactions on Multimedia*, 25:4610–4622, 2022.

- [53] Xiaogang Wang. Intelligent multi-camera video surveillance: A review. *Pattern recognition letters*, 34(1):3–19, 2013.
- [54] Mikołaj Wieczorek, Barbara Rychalska, and Jacek Dąbrowski. On the unreasonable effectiveness of centroids in image retrieval. In *Neural Information Processing: 28th International Conference, ICONIP 2021, Sanur, Bali, Indonesia, December 8–12, 2021, Proceedings, Part IV 28*, pages 212–223. Springer, 2021.
- [55] Fei Xiong, Mengran Gou, Octavia Camps, and Mario Sznaier. Person re-identification using kernel-based metric learning methods. In *Computer Vision–ECCV 2014: 13th European Conference, Zurich, Switzerland, September 6–12, 2014, Proceedings, Part VII 13*, pages 1–16. Springer, 2014.
- [56] Zhongcong Xu, Jianfeng Zhang, Jun Hao Liew, Hanshu Yan, Jia-Wei Liu, Chenxu Zhang, Jiashi Feng, and Mike Zheng Shou. Magicanimate: Temporally consistent human image animation using diffusion model. *arXiv preprint arXiv:2311.16498*, 2023.
- [57] Mang Ye, Jianbing Shen, Gaojie Lin, Tao Xiang, Ling Shao, and Steven CH Hoi. Deep learning for person re-identification: A survey and outlook. *IEEE transactions on pattern analysis and machine intelligence*, 44(6):2872–2893, 2021.
- [58] Hong-Xing Yu, Ancong Wu, and Wei-Shi Zheng. Unsupervised person re-identification by deep asymmetric metric embedding. *IEEE transactions on pattern analysis and machine intelligence*, 42(4):956–973, 2018.
- [59] Jiahui Yu, Xin Li, Jing Yu Koh, Han Zhang, Ruoming Pang, James Qin, Alexander Ku, Yuanzhong Xu, Jason Baldridge, and Yonghui Wu. Vector-quantized image modeling with improved vqgan. *arXiv preprint arXiv:2110.04627*, 2021.
- [60] Polina Zablotskaia, Aliaksandr Siarohin, Bo Zhao, and Leonid Sigal. Dwnet: Dense warp-based network for pose-guided human video generation. *arXiv preprint arXiv:1910.09139*, 2019.
- [61] Lvmin Zhang, Anyi Rao, and Maneesh Agrawala. Adding conditional control to text-to-image diffusion models. In *Proceedings of the IEEE/CVF International Conference on Computer Vision*, pages 3836–3847, 2023.
- [62] Zhilu Zhang and Mert Sabuncu. Generalized cross entropy loss for training deep neural networks with noisy labels. *Advances in neural information processing systems*, 31, 2018.
- [63] Haiyu Zhao, Maoqing Tian, Shuyang Sun, Jing Shao, Junjie Yan, Shuai Yi, Xiaogang Wang, and Xiaoou Tang. Spindle net: Person re-identification with human body region guided feature decomposition and fusion. In *2017 IEEE Conference on Computer Vision and Pattern Recognition (CVPR)*. IEEE, 2017.
- [64] Rui Zhao, Wanli Ouyang, and Xiaogang Wang. Unsupervised saliency learning for person re-identification. In *2013 IEEE Conference on Computer Vision and Pattern Recognition*, 2013.
- [65] Liang Zheng, Liyue Shen, Lu Tian, Shengjin Wang, Jingdong Wang, and Qi Tian. Scalable person re-identification: A benchmark. In *Computer Vision, IEEE International Conference on Computer Vision*, pages 1116–1124, 2015.
- [66] Liang Zheng, Yi Yang, and Alexander G Hauptmann. Person re-identification: Past, present and future. *arXiv preprint arXiv:1610.02984*, 2016.
- [67] Liang Zheng, Yi Yang, and Qi Tian. Sift meets cnn: A decade survey of instance retrieval. *IEEE transactions on pattern analysis and machine intelligence*, 40(5):1224–1244, 2017.
- [68] Wei-Shi Zheng, Shaogang Gong, and Tao Xiang. Person re-identification by probabilistic relative distance comparison. In *CVPR 2011*, pages 649–656. IEEE, 2011.
- [69] Zhedong Zheng, Xiaodong Yang, Zhiding Yu, Liang Zheng, Yi Yang, and Jan Kautz. Joint discriminative and generative learning for person re-identification. In *proceedings of the IEEE/CVF conference on computer vision and pattern recognition*, pages 2138–2147, 2019.
- [70] Zhedong Zheng, Liang Zheng, and Yi Yang. Unlabeled samples generated by gan improve the person re-identification baseline in vitro. In *2017 IEEE International Conference on Computer Vision (ICCV)*. IEEE, 2017.
- [71] Zhedong Zheng, Liang Zheng, and Yi Yang. Unlabeled samples generated by gan improve the person re-identification baseline in vitro. In *Proceedings of the IEEE International Conference on Computer Vision*, pages 3754–3762, 2017.

- [72] Z Zhong, L Zheng, Z Zheng, S Li, and Y Yang. Camera style adaptation for person re-identification. In *Proceedings of the IEEE Computer Society Conference on Computer Vision and Pattern Recognition*, 2018.
- [73] Zhun Zhong, Liang Zheng, Guoliang Kang, Shaozi Li, and Yi Yang. Random erasing data augmentation. In *Proceedings of the AAAI Conference on Artificial Intelligence*, volume 34, pages 13001–13008, 2020.
- [74] Kuan Zhu, Haiyun Guo, Shiliang Zhang, Yaowei Wang, Jing Liu, Jinqiao Wang, and Ming Tang. Aaformer: Auto-aligned transformer for person re-identification. *IEEE Transactions on Neural Networks and Learning Systems*, 2023.
- [75] Shenhao Zhu, Junming Leo Chen, Zuozhuo Dai, Yinghui Xu, Xun Cao, Yao Yao, Hao Zhu, and Siyu Zhu. Champ: Controllable and consistent human image animation with 3d parametric guidance. *arXiv preprint arXiv:2403.14781*, 2024.

A Additional Qualitative Results

In this section, we present additional qualitative results produced by our framework, Diff-ID. Each subsection highlights different categories of generated images.

A.1 Generated images with of out-of-domain human pose distributions

Given a reference image in the training dataset, which is DukeMTMC-reID [71] and Market-1501 [65], we sampled various human poses from the Everybody Dance Now dataset [4]. We generated images that preserve the identity of the reference image while adopting human poses sourced from outside the training dataset. Fig. 8 demonstrates that the proposed model exhibits noticeable generalization ability and high-quality image generation.



Figure 8: **Generated images with out-of-domain human poses.** We show the generation results with diverse human poses.

A.2 Generated images with various camera elevations

We present the generation results with human poses captured at both high and low camera elevations. The human poses used as conditions for the generative model are extracted from the training dataset, with high elevation poses being relatively challenging. Fig. 9 illustrates how appearance and human poses vary with camera positions, particularly with changes in elevation, emphasizing the importance of data augmentation with diverse camera poses.



Figure 9: **Generated images with various elevations.** We generate images with high and low camera elevations. Ref. denotes the reference image.

A.3 Generated images with diverse poses

We generate images with diverse pose and identities for both Market-1501 [65] and DukeMTMC-reID [71] dataset. Fig. 10 demonstrates our framework’s capability to generate high-fidelity images that reproduce the identities of the reference images despite the diverse variations.



Figure 10: **Generated images with diverse poses.** We show additional qualitative results of the generated images. Ref. denotes the reference image.

A.4 Generated images with same poses

We generate images with same human poses and different identities for DukeMTMC-reID [71]. Diff-ID generates realistic images regardless of how human pose conditions are different from human poses of reference images. In Fig. 11, the first column of generated images demonstrates our framework’s capability to generate images despite extreme human poses.

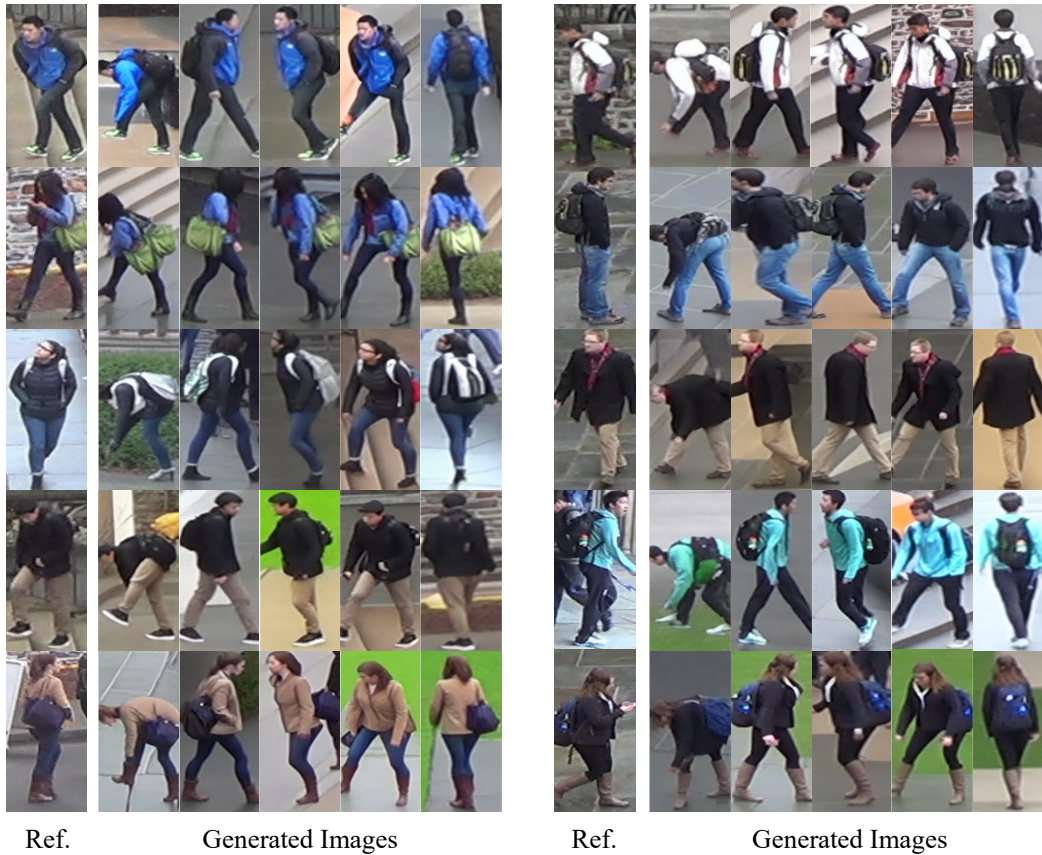


Figure 11: **Generated images with same poses.** We generate images with same human pose and different identities. Ref. denotes the reference image.